Supporting Information

Efficient and convenient strategy for recovering hexavalent chromium ions from wastewater by a novel photocatalytic iron-based metal-organic frameworks mesh

Yu Gao[1,2,3], Siyu Liu[1,2,3], Xu Huang[1,2,3], Weiwen Lu[1,2,3], Jian Huang[1,2,3], Hua Zhang[1,2,3], Yong Zhang[1,2,3], Jinhua Wang[1,2,3], Shanshan Xi[1,2,3], Jun Liu[4], Tao Luo[1,2,3*]

1 Anhui Institute of Ecological Civilization, Anhui Jianzhu University, Hefei, Anhui 230601, PR China

2 Anhui Provincial Key Laboratory of Environmental Pollution Control and Resource Reuse, Anhui Jianzhu University, Hefei, Anhui 230601, PR China.

3 School of Environment and Energy Engineering, Anhui Jianzhu University, Hefei, Anhui 230601, PR China.

4 Pollution Control and Resource Utilization in Industrial Parks Joint Laboratory of Anhui Province, Anhui Zhonghuan Environmental Protection Technology CO. LTD, Hefei, Anhui 230051, PR China.

* To whom correspondence should be addressed:
luotao_edu@163.com (Tao Luo)

1. Synthesis of the photocatalysts

1.1 Synthesis of Fe@MIL-53(Fe) and Fe@MIL-101(Fe)

Fe@MIL-53(Fe) was prepared according to previously reported literature.[1] 0.8100 g 1, 4-benzenedicarboxylic acid and 50 mL DMF were mixed in a beaker. Then, the mixture kept magnetic stirring at room temperature for 3 h. Subsequently, three pieces of iron network (the iron network was cleaned for three times with methanol in an ultrasonic cleaner to remove impurities) were placed into a 100 mL Teflon liner. After adding 3 mL hydrochloric acid, the mixture was put in stainless steel reactor. The reaction system was transferred into the oven and heated at 170 °C for 24 h. After nature cooling, the networks were washed with DMF and ethanol for three times. Finally, the products were vacuum dried under 60 °C for several hours.

Fe@MIL-101(Fe) was synthesized by a hydrothermal method. 0.600 g 1, 4-benzenedicarboxylic acid and 55 mL DMF were mixed in a beaker. Then, the mixture kept magnetic stirring at room temperature for 3 h. Subsequently, three pieces of iron mesh were placed into a 100 mL Teflon liner. After adding 3 mL hydrochloric acid, the mixture was put in stainless steel reactor. The reaction system was transferred into the oven and heated at 150 °C for 12 h. After nature cooling, the networks were washed with DMF and ethanol for three times. Finally, the products were vacuum dried under 60 °C for several hours.

1.2 Synthesis of Fe@NH_2-MIL-53(Fe) and Fe@NH_2-MIL-101(Fe)

Fe@NH_2-MIL-53(Fe) and Fe@NH_2-MIL-101(Fe) were obtained by replacing H_2BDC with NH_2-H2BDC while keeping all other synthetic conditions unchanged.

1.3 Synthesis of Fe@MIL-100(Fe)

The synthetic method of in-situ grown Fe@MIL-100(Fe) was improved on the basis of the experimental method described in the literature.[1-4] First, three pieces of the Iron network (3cm×3cm) was washed for three times with methanol and Milli-Q water in an ultrasonic cleaner to eliminate the organic matter and impurities. Then, the 0.900 g 1,3,5-benzenetricarboxylic acidand 60 ml Milli-Q water were mixed. The solution was stirred at room temperature for 3 h，and transferred into a 100 mL teflon-liner. After adding 3 mL hydrochloric acid, mixed into the solution, the reaction system was transferred into in stainless steel reactor and heated at 140 °C for 24 h. At the end of the reaction, the reactor was cooled to room temperature, the products were immersed in Milli-Q water for 3 h. Finally, the sample was vacuum dried at 60 °C for 12 h to obtain Fe@MIL-100(Fe)

The synthesis routes for the five samples are illustrated in Scheme S2.

1.4 Characterization techniques

The crystal phase structures of all samples were identified via X-ray diffraction (XRD, Smart Lab SE), provided with the Cu Kα radiation (40kV, 100mA). The morphologies and structures of the samples were attained from a scanning electron microscopy (SEM, JSM-7500F). The functional groups on the samples were detected via a Fourier transform infrared microscope (FITR-650) by uniformly dispersing the powder on the surface of the samples in potassium bromide. The surface chemical composition and electronic states of samples were collected on an X-ray photoelectron spectrometer (XPS, Thermo ESCALAB 250Xi) spectrum The UV-visible diffuse-

reflectance spectra (UV-vis DRS, SolidSpec-3700) of the samples were recorded in the wavelength range of 200-800 nm with barium sulfate as reference. The photoluminescence (PL, F-4700) spectra were investigated to the light absorption of the as-prepared samples. The specific surface areas and pore volume of the photocatalysts were performed on a Brunauer-Emmett-Teller (BET, ASAP-2460) at 77 K. The zeta potentials of sample under different pH values were determined by a Zeta-sizer Nano-ZS analyzer at room temperature. Inductively Coupled Plasma (ICP, Optima 8000) analysis was performed for measurement of leaching amount of Fe from catalyst to solution and Cr(III) concentration in solution after photocatalytic reaction.

1.5 Self- manufactured Cr(VI) recovery system

To enhance the utilization efficiency of the prepared mesh materials and achieve the recovery of Cr(VI), a circulating reactor was designed for the photocatalytic reduction and recovery of Cr(VI) (Scheme S1). This design aims to address the efficient reduction and resourceful recovery of Cr(VI) using photocatalytic membrane materials. The setup consists of several components, including a reaction tank, an alkali tank, an acid tank, and a connecting assembly. The connecting assembly comprises a peristaltic pump and connecting pipes. The peristaltic pump and connecting pipes are connected to the reaction tank, alkali tank, and acid tank, respectively, forming a circulatory system. This configuration enables the circulation of the reaction solution through the various tanks, facilitating the efficient reduction of Cr(VI) and its subsequent recovery.

2. List of figures and tables

(1); alkali tank (2); acid tank (3); connected components (4); automatic dosing system (5); peristaltic pumps (41); connection pipe (42).

Scheme S2. The synthetic route of five Fe@MILs mesh.

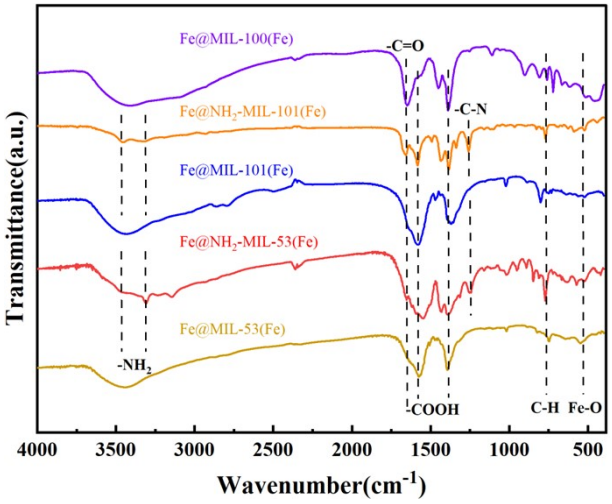

Figure. S1 FT-IR spectra of the five samples.

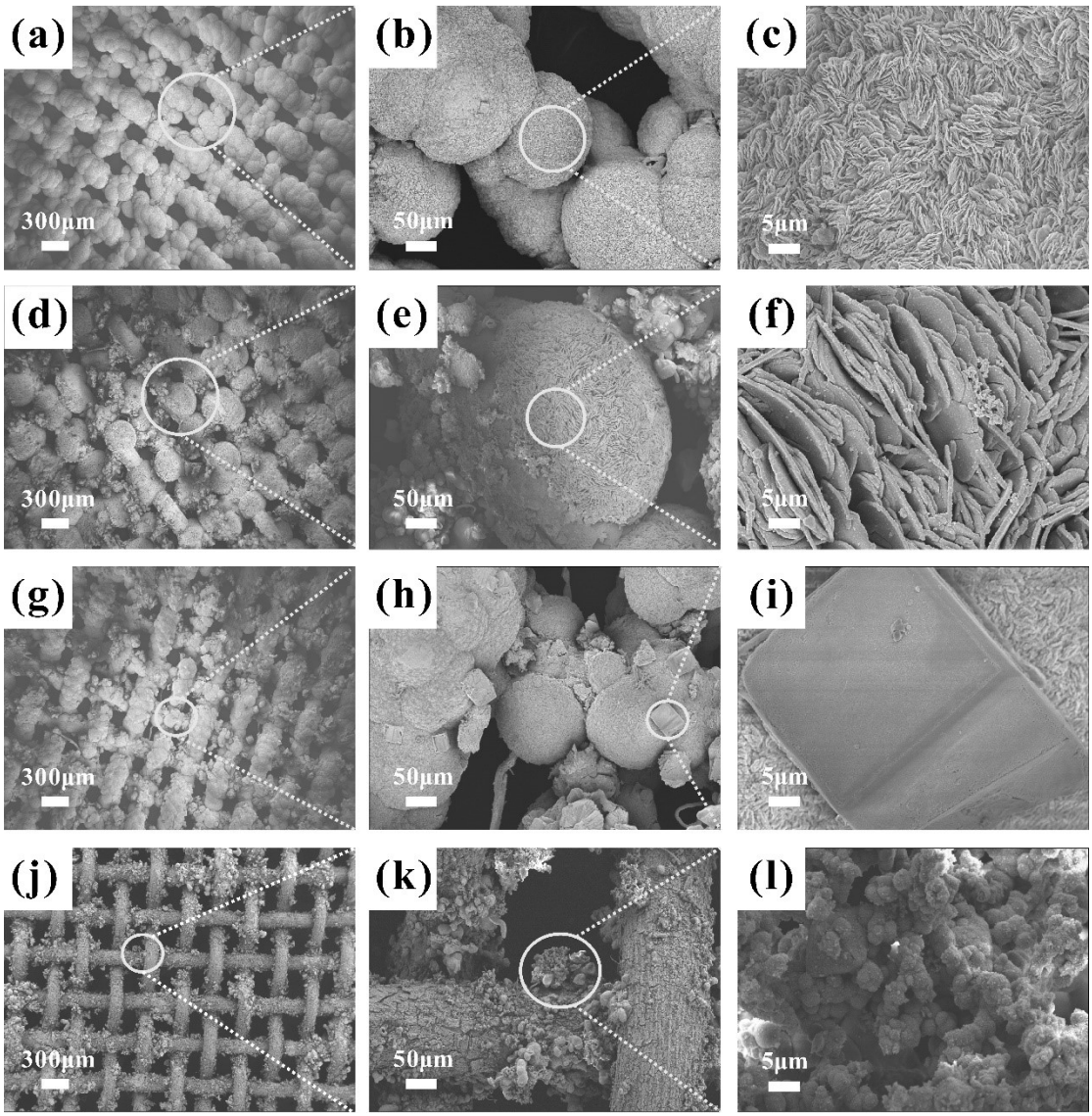

Figure. S2 SEM images of Fe@MIL-53(Fe) (a-c); SEM images of Fe@NH_2-MIL-53(Fe) (d-f); SEM images of Fe@MIL-101(Fe) (g-i); SEM images of Fe@NH_2-MIL-101(Fe) (j-l).

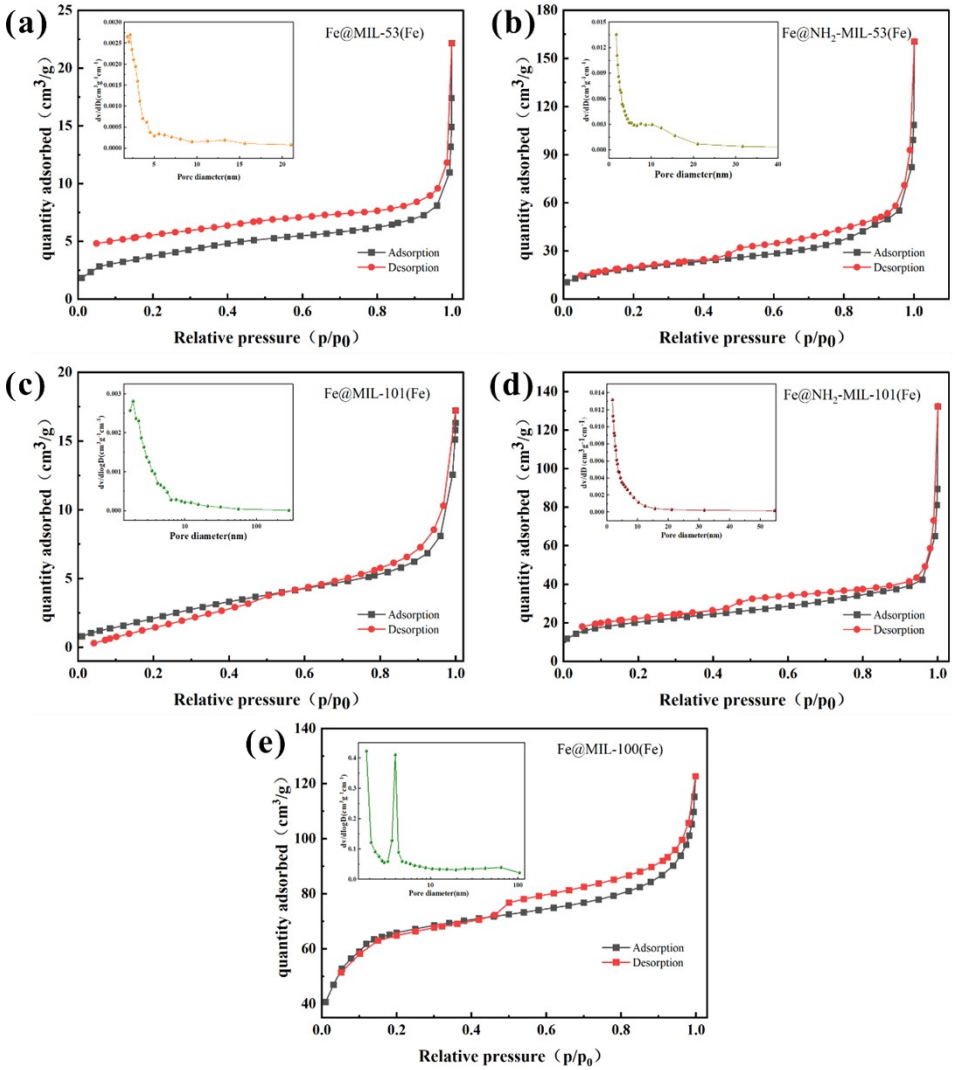

Figure. S3 N_2 adsorption-desorption isotherms and pore size distributions of Fe@MIL-53(Fe) (a); N_2 adsorption-desorption isotherms and pore size distributions of Fe@NH_2-MIL-53(Fe) (b); N_2 adsorption-desorption isotherms and pore size distributions of Fe@MIL-101(Fe) (c); N_2 adsorption-desorption isotherms and pore size distributions of Fe@NH_2-MIL-101(Fe) (d); N_2 adsorption-desorption isotherms and pore size distributions of Fe@MIL-100(Fe) (e).

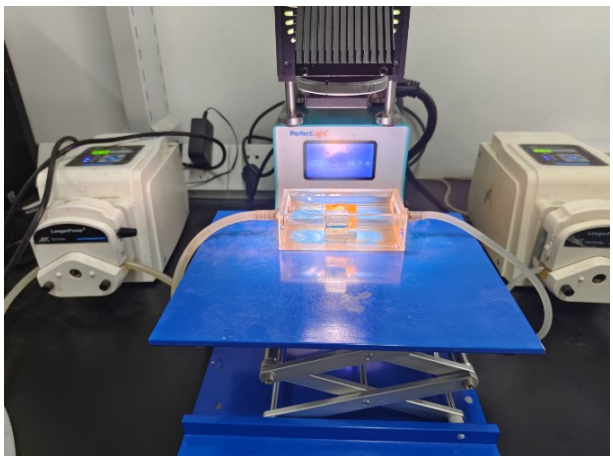

Figure. S4 Digital image of the photocatalytic reactor.

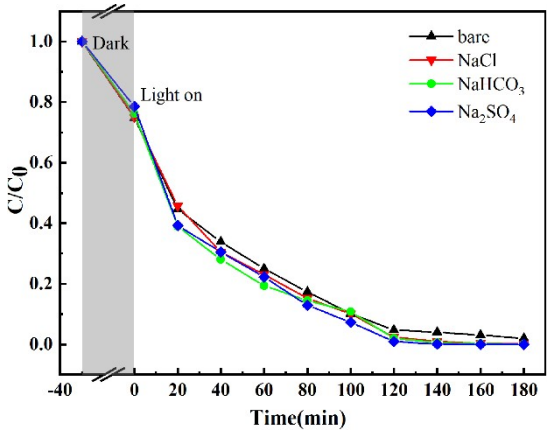

Figure. S5 Reduction of Cr(VI) at different co-existing ions.

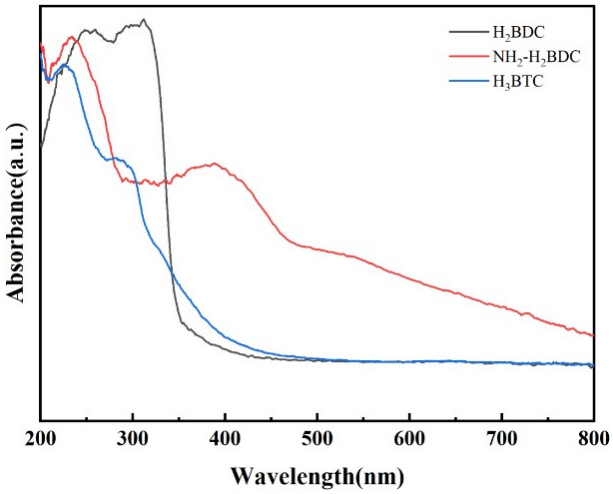

Figure. S6 UV–vis DRS diffuse reflectance spectra of ligands.

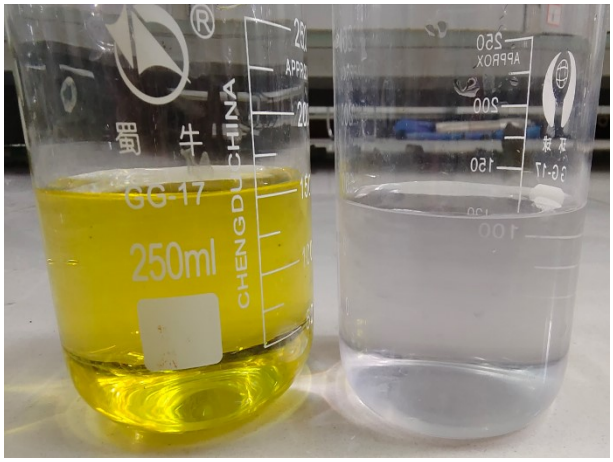

Figure. S7 Cr solutions before and after the reaction.

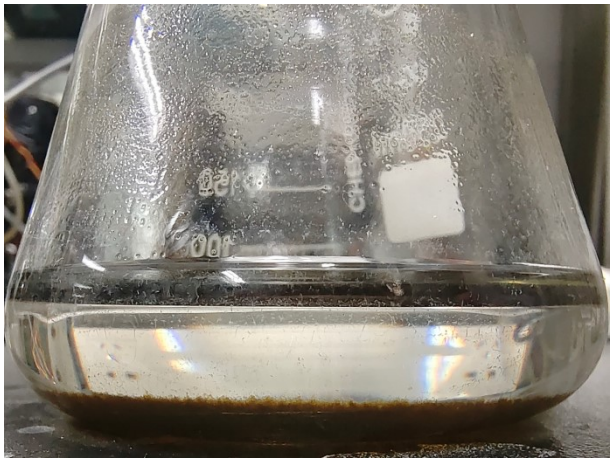

Figure. S8 $Cr(OH)_3$ deposition.

Table S1. Comparison of the photocatalytic reduction of hexavalent chromium by different MOFs.

Photocatalyst	Form	Concentration (mg/L)	Removal efficiency (%)	Ref
MIL-100(Fe)	powder	4.2	43.1	[5]
MIL-53(Fe)	powder	20	100	[6]
NH_2-MIL-53(Fe)	powder	20	49	[7]
MIL-101(Fe)	powder	8	100	[8]
NH_2-MIL-101(Fe)	powder	20	51	[9]
Fe@MIL-53(Fe)	mesh	50	49.4	This work
Fe@NH_2-MIL-53(Fe)	mesh	50	53.4	This work
Fe@MIL-101(Fe)	mesh	50	48.5	This work
Fe@NH_2-MIL-101(Fe)	mesh	50	58.1	This work
Fe@MIL-100(Fe)	mesh	50	98	This work

Table S2. The leaching Fe during the photocatalytic reactions were determined by ICP-OES.

Cycles	The concentration of Fe (μg/L)
1	48.91
2	36.65
3	19.74
4	22.12
5	15.37

Table S3. The reacted solution was determined by ICP-OES and UV spectrophotometer.

concentration	(mg/L)
Total Cr	47.42
Cr(VI)	1.25
Cr(III)	46.17

Table S4. The Cr(III) concentration in supernatant after dropwise addition of different volume of 1mol/L NaOH.

NaOH volume (mL)	Cr(III) concentration in supernatant (mg/L)
0	46.17
1	19.686
3	10.228
5	1.268

Cr(VI) recovery:

$$\text{Efficiency (\%)} = \frac{V_0 - V_1}{V_0}$$

where V_0 is the Cr(III) concentration in supernatant without NaOH addition, V_1 is Cr(III) concentration in the supernatant after addition of different concentrations of NaOH.

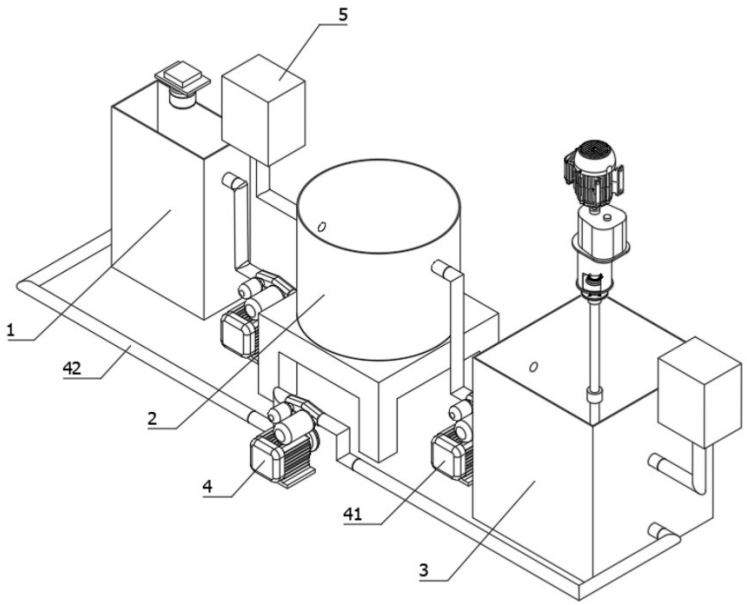

Scheme S1. Self- manufactured Cr(VI) recovery system: photocatalytic reaction tank (1); alkali tank (2); acid tank (3); connected components (4); automatic dosing system (5); peristaltic pumps (41); connection pipe (42).

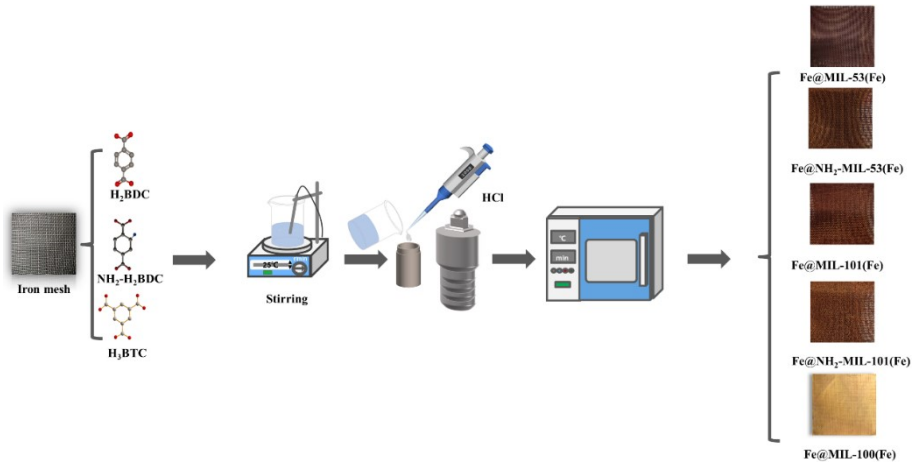

Scheme S2. The synthetic route of five Fe@MILs mesh.

References

[1] W. Li, J. Cao, W. Xiong, Z. Yang, S. Sun, M. Jia, Z. Xu, In-situ growing of metal-organic frameworks on three-dimensional iron network as an efficient adsorbent for antibiotics removal, Chemical Engineering Journal, 392 (2020) 124844.

[2] G. Li, J. Li, S. Zhang, X. Hou, X. Liu, Q. Yu, M. Li, In-situ growing of metal-organic frameworks on iron mesh as a recyclable remediation material for removing hexavalent chromium from groundwater, Chemosphere, 303 (2022) 135187.

[3] J. An, Y. Li, W. Chen, G. Li, J. He, H. Feng, Electrochemically-deposited PANI on iron mesh-based metal-organic framework with enhanced visible-light response towards elimination of thiamphenicol and E. coli, Environmental Research, 191 (2020) 110067.

[4] D. Wang, S.E. Gilliland, III, X. Yi, K. Logan, D.R. Heitger, H.R. Lucas, W.-N. Wang, Iron Mesh-Based Metal Organic Framework Filter for Efficient Arsenic Removal, Environmental Science & Technology, 52 (2018) 4275-4284.

[5] L. Wang, K. Zhang, J. Qian, M. Qiu, N. Li, H. Du, X. Hu, Y. Fu, M. Tan, D. Hao, Q. Wang, S-scheme MOF-on-MOF heterojunctions for enhanced photo-Fenton Cr(VI) reduction and antibacterial effects, Chemosphere, 344 (2023) 140277.

[6] R. Liang, F. Jing, L. Shen, N. Qin, L. Wu, MIL-53(Fe) as a highly efficient bifunctional photocatalyst for the simultaneous reduction of Cr(VI) and oxidation of dyes, Journal of Hazardous Materials, 287 (2015) 364-372.

[7] Y. Chen, Z. Yu, Q. Xiang, G. Yang, Q. Tan, N. He, S. Guo, Y. Liu, Z-scheme heterojunction Bi2WO6/NH2-MIL-53(Fe) photocatalyst: Simultaneous efficient photo-Fenton degradation of SMX and photocatalytic reduction of Cr(VI), Materials Science in Semiconductor Processing, 170 (2024) 107966.

[8] B. Liu, Y. Wu, X. Han, J. Lv, J. Zhang, H. Shi, Facile synthesis of g-C3N4/amine-functionalized MIL-101(Fe) composites with efficient photocatalytic activities under visible light irradiation, Journal of Materials Science: Materials in Electronics, 29 (2018) 17591-17601.

[9] D. Pattappan, K.V. Kavya, S. Vargheese, R.T.R. Kumar, Y. Haldorai, Graphitic carbon nitride/NH2-MIL-101(Fe) composite for environmental remediation: Visible-light-assisted photocatalytic degradation of acetaminophen and reduction of hexavalent chromium, Chemosphere, 286 (2022) 131875.